Equilibrium electro-osmotic instability in concentration polarization at a perfectly charge-selective interface

I. Rubinstein* and B. Zaltzman†
Blaustein Institutes for Desert Research, Ben-Gurion University of the Negev, Sede Boqer Campus 8499000, Israel
(Received 4 March 2017; published 27 September 2017)

Equilibrium electroconvective instability at a perfectly charge-selective solid, such as ion-exchange membrane or metal electrode, previously deemed impossible, is possible if one takes into account finite electrical conductivity of the solid. A simple model of electroconvective diffusion of ions in the depleted diffusion layer in this system predicts a supercritical transition to instability in the vicinity of the limiting current, as opposed to the subcritical transition for the previously studied nonequilibrium instability related to the extended space charge. The linear stability analysis in this model yields the division of the parameter space into domains in which each instability mechanism with its characteristic signatures dominates. Identification of the particular instability mechanism for a given system requires a detailed experimental study of the vicinity of the instability threshold in terms of both the voltage versus current dependence and flow visualization.

DOI: 10.1103/PhysRevFluids.2.093702

I. INTRODUCTION

It has been recently shown that, for a nonperfectly charge-selective interface, equilibrium electroconvective instability in ionic concentration polarization may occur due to lateral variations of the interface electrochemical potential of counterions [1]. Previously, for a perfect interface, this was deemed impossible [2], leaving the nonequilibrium instability as the only possibility. This consideration was based on the assumption made in the existing models that perfect charge selectivity is tantamount to assuming a fixed counterion concentration at the interface (equal to the high concentration of fixed charges) along with its infinite conductivity. Taken together, both imply a vanishing lateral variation of the electrochemical potential of counterions in the interface. In practice, the charge-selective solids, e.g., ion-exchange electrodialysis membranes, indeed are highly, essentially perfectly, charge selective (permselective). At the same time their conductivity is by no means infinite. In this paper we propose a simple model of locally electroneutral equilibrium ion transfer through a perfectly charge-selective membrane with a finite lateral conductivity and show that quiescent concentration polarization at such a membrane is unstable above a realistic voltage threshold. We indicate a system parameter range in which equilibrium and nonequilibrium instability mechanisms dominate and characteristic experimental signatures of both. We hope that this finally sets an adequate framework for much needed future experimental investigation of this still relatively novel and understudied interface-driven hydrodynamic instability.

The one-dimensional (1D) passage of a dc electric current from an electrolyte solution into a charge-selective solid is hydrodynamically unstable [3–10]. The resulting vortical flow in the depleted diffusion layer yields overlimiting conductance through such solids [11]. For a long time, this instability has been either explicitly or implicitly attributed to nonequilibrium electro-osmosis [12–14], related to the extended space charge [15–18], which develops in the course of the ionic concentration polarization at the limiting current [19–23]. This amounted to studying various time-dependent and nonlinear features of electro-osmotic instability for a

*robinst@post.bgu.ac.il
†boris@bgu.ac.il

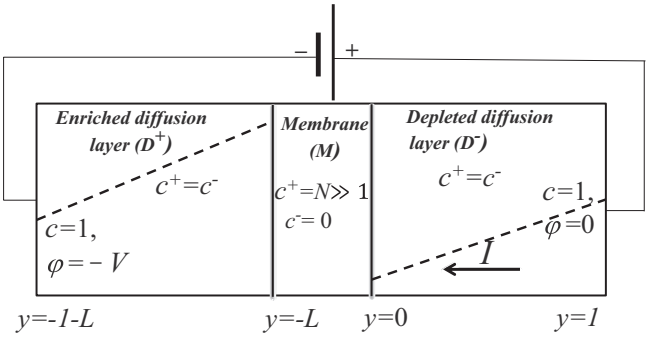

FIG. 1. Scheme of the three-layer setup. Dashed lines mark schematic plots of the average ionic concentration $C(y)$.

perfectly charge-selective interface at constant uniform electric potential, implying a laterally uniform counterion electrochemical potential of the interface [3–6,13,24–27].

Recently [1], we showed that any deviation from constancy of the electrochemical potential of counterions at the outer edge of electric double layer (EDL) makes equilibrium instability possible, driven by either equilibrium electro-osmosis or bulk electroconvection, or both. Nonconstancy of the counterionic electrochemical potential may result either from nonideal permselectivity of the interface, addressed in [1], or from any other source, e.g., a finite rate of electrode reactions in cathodic deposition of a metal from its salt solution. In this paper we identify another source of lateral variation of electrochemical potential of counterions: finite conductivity of a perfectly permselective ion-exchange membrane. (In practice, the unit area resistance of commercial cation-exchange membranes varies in the range from 1 to 100 $\Omega\,\mathrm{cm}^2$ for a counterion transport number of about 0.98 corresponding to essentially perfect permselectivity).

II. MODELING CONCENTRATION POLARIZATION AT A PERFECTLY CHARGE-SELECTIVE SOLID OF FINITE CONDUCTIVITY

To analyze the possible effect of finite conductivity of a perfectly permselective membrane upon the hydrodynamic stability in concentration polarization we propose the following simple model. Let us consider a three-layer system consisting of an infinite 2D cation-exchange membrane M, with $-\infty < x < \infty$ and $-L < y < 0$, flanked by two diffusion layers D^+ and D^-, with $-\infty < x < \infty$ and $-1 - L < y < -L$ and with $-\infty < x < \infty$ and $0 < y < 1$, respectively, of a univalent electrolyte with concentration c_0 maintained at the outer boundaries of the diffusion layers (see Fig. 1).

Since the electroconvection phenomenon we wish to explore is related to the high electric field that forms in the course of concentration polarization in the depleted diffusion layer, it is natural to restrict our flow analysis to this layer only while disregarding as a first approximation the minor possible electro-osmotic transmembrane flow along with that in the enriched diffusion layer. This three-layer system is modeled by the following boundary-value problem, nondimensionalized in a natural manner [13,14,28–30]:

$$\frac{\partial c_\pm}{\partial t} = -\nabla \cdot \mathbf{j}_\pm, \tag{1}$$

$$\mathbf{j}_\pm = -D(y)c_\pm \nabla \mu_\pm - \mathrm{Pe}\mathbf{v}c_\pm, \quad \mu_\pm = \ln c_\pm \pm \varphi. \tag{2}$$

Here $c_\pm$ is the concentration of positive and negative ions, Pe is the material Péclet number [26], and $D(y)$ is a relative diffusivity, equal to unity in the diffusion layers and to $D \ll 1$ in the membrane. Electroneutrality conditions in the enriched, $-1 - L < y < -L$, and in the depleted, $0 < y < 1$,

diffusion layers and in the membrane, $-L < y < 0$, read, respectively,

$$c_+ = c_- = C, \quad -L-1 < y < -L, 0 < y < 1; \tag{3}$$

$$c_+ = c_- + N, \quad -L < y < 0. \tag{4}$$

Here N is the dimensionless fixed charge density in the membrane (scaled by ec_0) and $C = (c_+ + c_-)/2$ is the average ionic concentration. The system (1)–(4) is complemented by boundary or interface conditions specifying the ionic concentrations and electric potential in the reservoir and prescribing continuity of ionic fluxes and electrochemical potential at the membrane-solution interfaces.

In typical ion-exchange membranes the ionic diffusivity is about one order of magnitude lower than that in solution, whereas the fixed charge concentration is at least one order of magnitude higher than the bulk electrolyte concentration. Then the case of a perfectly permselective solid of finite conductivity corresponds to the asymptotic limit $\sigma = DN = O(1)$, $D \ll 1$, and $N \gg 1$, where σ is the membrane conductivity. In this case the three-layer model (1)–(4) is reduced to the following asymptotic limit:

$$\frac{\partial C}{\partial t} + \mathrm{Pe}\mathbf{v}\cdot\nabla C = \nabla\cdot(\nabla C \pm C\nabla\varphi) \text{ in } D^{\pm}; \tag{5}$$

$$\sigma\nabla^2\varphi = 0 \text{ in } M; \tag{6}$$

$$C_y - C\varphi_y|_{D^{\pm}} = 0, \quad C_y + C\varphi_y|_{D^{\pm}} = \sigma\varphi_y|_M \quad \text{for the } M\text{-}D^{\pm} \text{ interface}, \quad y = -L, 0 \tag{7}$$

$$\ln C + \varphi|_{D^{\pm}} = \ln N + \varphi|_M. \tag{8}$$

Here (5) are convection-diffusion equations for counterions and co-ions in the diffusion layer, (6) is the equation for electric potential in the perfectly permselective membrane of finite conductivity σ, and (7) and (8) are, respectively, conditions of vanishing normal co-ion flux, continuity of normal counterion flux, and continuity of the counterionic electrochemical potential μ_+ across the membrane-solution interfaces $y = -L, 0$. As mentioned previously, we neglect the fluid flow in the enriched diffusion layer and in the membrane, $\mathbf{v} = u\mathbf{i} + w\mathbf{j} \equiv 0$ and $y < 0$, and determine it in the depleted diffusion layer from the Stokes-continuity equations:

$$\nabla^2\mathbf{v} - \nabla p + \nabla^2\varphi\nabla\varphi = 0, \quad \nabla\cdot\mathbf{v} = 0. \tag{9}$$

At the membrane–depleted diffusion layer interface M-D^-, $y = 0$, we apply the equilibrium electro-osmotic slip condition

$$u = \zeta\left(\varphi_x + \frac{C_x}{C}\right) + \frac{C_x}{C}[4\ln 2 - 4\ln(e^{\zeta/2} + 1)], \tag{10}$$

where $\zeta = \ln[C(x,0,t)/N]$ is the dimensionless electric potential drop between the interface and the outer edge of the EDL. This expression, derived in [14,31], results from accounting for polarization of the EDL by the applied tangential field, resulting, in particular, in major lateral pressure drops in the double layer, owing to the lateral variation of the Maxwell stresses.

At the outer boundary of the depleted diffusion layer we apply the reservoir conditions for velocity $u_y(x,1) = 0$ and $w(x,1) = 0$, along with prescribing the concentration and the electric potential at the outer edges of both diffusion layers:

$$C|_{y=1} = 1, \quad \varphi|_{y=-L-1} = -V, \quad \varphi|_{y=1} = 0. \tag{11}$$

The main control parameters are the dimensionless voltage V, the dimensionless width of the membrane L, and membrane's conductivity σ.

III. LINEAR STABILITY ANALYSIS OF THE QUIESCENT STATE AND EQUILIBRIUM ELECTRO-OSMOTIC INSTABILITY

Integration of the three-layer problem (1)–(4) yields the following expressions for its quiescent 1D steady-state solution:

$$C = 1 - \frac{J}{2}(y + L + 1), \quad \varphi = \frac{I}{J}\ln C - V \quad \text{for } -L-1 < y < -L; \tag{12}$$

$$C = 1 - \frac{J}{2}(y - 1), \quad \varphi = \frac{I}{J}\ln C, \quad \text{for } 0 < y < 1; \tag{13}$$

$$\begin{gathered} C + \frac{NI}{2J}\ln\left[C + \frac{N}{2}\left(1 - \frac{I}{J}\right)\right] = -\frac{J}{2D}y + A \quad \text{for } -L < y < 0; \\ 2C + N\varphi = -\frac{J}{D}y + B. \end{gathered} \tag{14}$$

Integration constants A and B, 1D current density $I = j_+ - j_-$, and salt flux $J = j_+ + j_-$ are found from continuity of electrochemical potentials across the membrane-solution interfaces $y = -L, 0$. Similarly, integration of the limit problem (5)–(9) yields

$$I = J = j_+; \tag{15}$$

$$C = 1 - J(y + L + 1),\ \varphi = \ln C - V \quad \text{for } -L-1 < y < -L; \tag{16}$$

$$C = 1 - J(y - 1),\ \varphi = \ln C \quad \text{for } 0 < y < 1; \tag{17}$$

$$\varphi = -\frac{J}{\sigma}(y + L) + 2\ln\left(1 - \frac{J}{2}\right) - V \quad \text{for } L < y < 0, \tag{18}$$

where the 1D steady-state current $I = J$ is related to voltage through

$$V = 2\ln\frac{2 - J}{2 + J} - \frac{JL}{\sigma}. \tag{19}$$

In Fig. 2(a) we present the corresponding voltage-current dependence in the solution (12)–(14) for a fixed σ and an increasing sequence of N converging to the limiting voltage-current curve (19) (in the general 2D case current density $\mathbf{I}$ is defined as $\mathbf{I} = \mathbf{j}^+ - \mathbf{j}^-$ and I is the normal component of $\mathbf{I}$ averaged over the interface).

The linear stability of the solution (15)–(19) is analyzed for the following setups. The first setup allows for bulk electroconvection [flow due to the residual space charge as represented by the electric force term in (9)] in the depleted diffusion layer D^-, combined with the electro-osmotic slip as represented by condition (10) (the bulk electroconvection–electro-osmotic setup). The second setup considers solely equilibrium electro-osmotic slip [no electric force term in (9), the electro-osmotic setup]. The linear stability analysis of the solution (15)–(19) is carried out in a standard fashion. This includes linearization of the system (5)–(11) with respect to perturbations around the solution (15)–(19), followed by the separation of the time variable in the linearized system and Fourier transform in the x variable. This yields a Sturm-Liouville problem in terms of a set of ordinary differential equations (ODEs) for the Fourier transform of the perturbation amplitude and its growth rate as the spectral parameter. The spectral problem was solved using the MAPLE ODE solver. The results of this linear stability analysis are presented in Figs. 2(b) and 2(c). The region above the neutral stability curves on the V-k plane in Figs. 2(b) and 2(c) corresponds to instability. Whereas for a poorly selective solid the instability is driven by the bulk force due to the effect of lateral variation of the counterionic transport number in the system [32] for a perfectly permselective membrane, the latter vanishes and the bulk-force term stabilizes the 1D concentration polarization. Thus, the sole driving factor of instability is the equilibrium electro-osmotic slip. This is the reason why the

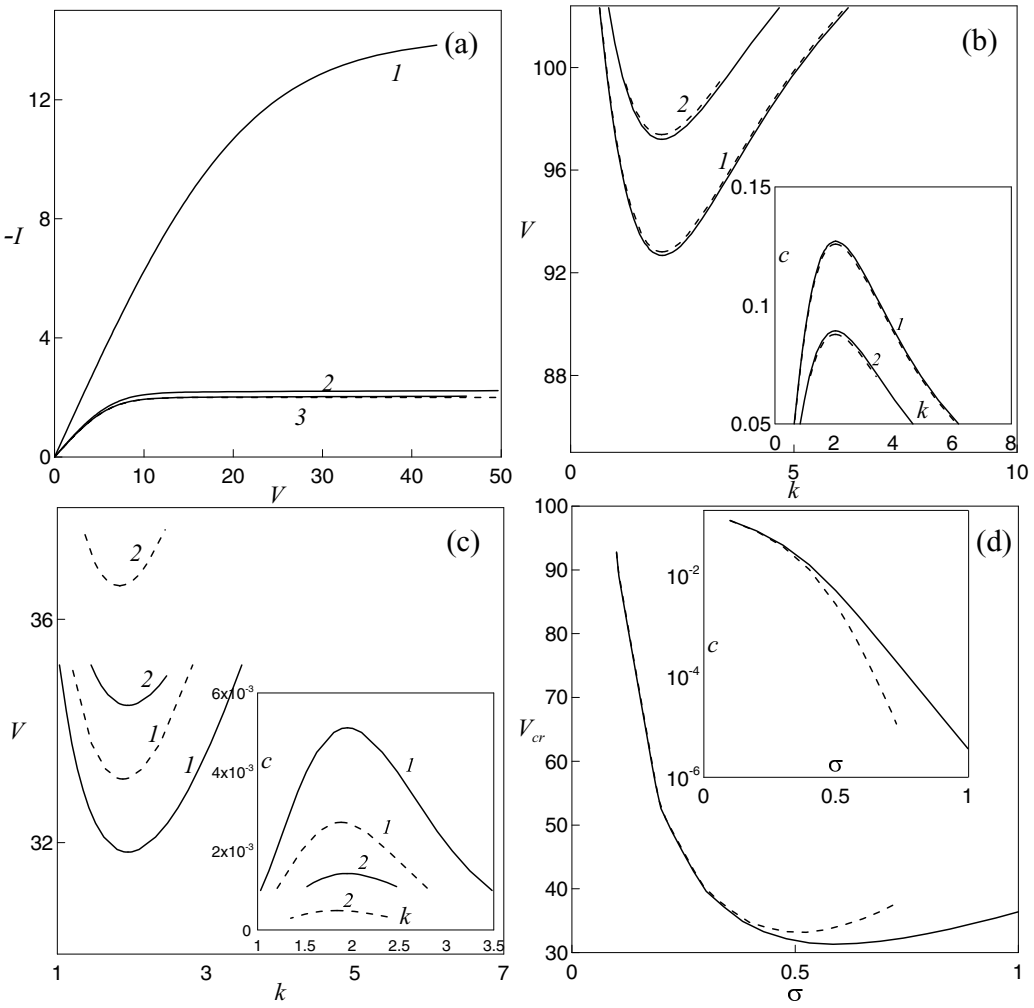

FIG. 2. (a) Voltage-current dependence for the 1D steady state in the model (1)–(4) (solid lines) and its perfectly selective membrane limit (5)–(11) (dashed line) for $L = 1$ and $\sigma = 1$: 1, $N = 1$; 2, $N = 10$; 3, $N = 100$. (b) Neutral stability curves in the V-k (wave number) plane (above the curve is instability) for a perfect membrane, for $L = 5$ and $\sigma = 0.1$: 1, $N = 100$; 2, $N = 25$. The solid line stands for the electro-osmotic setup and the dashed line for the bulk electroconvection-electro-osmotic setup. The inset is the same but for the minimum depleted interface electrolyte concentration in the c-k plane. (c) Same as (b) but for $\sigma = 0.5$. (d) Instability threshold in the V-σ plane for $L = 5$ and $N = 100$. The inset is the same but for the c-σ plane.

instability thresholds are sensitive to the variation of N through the dependence of the ζ potential on it [Eq. (10)]. On the other hand, the stabilizing effect of the bulk-force term increases with the increase of the membrane conductivity σ [Figs. 2(b) and 2(c)]. The dependence of the instability's voltage and the depleted interface concentration thresholds on conductivity are plotted in Fig. 2(d). We note that for a poorly conductive highly selective membrane the instability occurs for a minor degree of concentration polarization (low depletion) [inset in Fig. 2(b)], whereas for a higher conductivity the instability occurs for a very high depletion [insets in Figs. 2(c) and 2(d)]. In practice, the dimensionless control parameter σ varies in the range of 0.1–10 for a commercial cation-exchange membrane with a unit area resistance in the range of 1–100 $\Omega\,\mathrm{cm}^2$, for a strong electrolyte solution with resistivity of the order of 100 Ω cm, for a membrane's and diffusion layers' thickness varying in

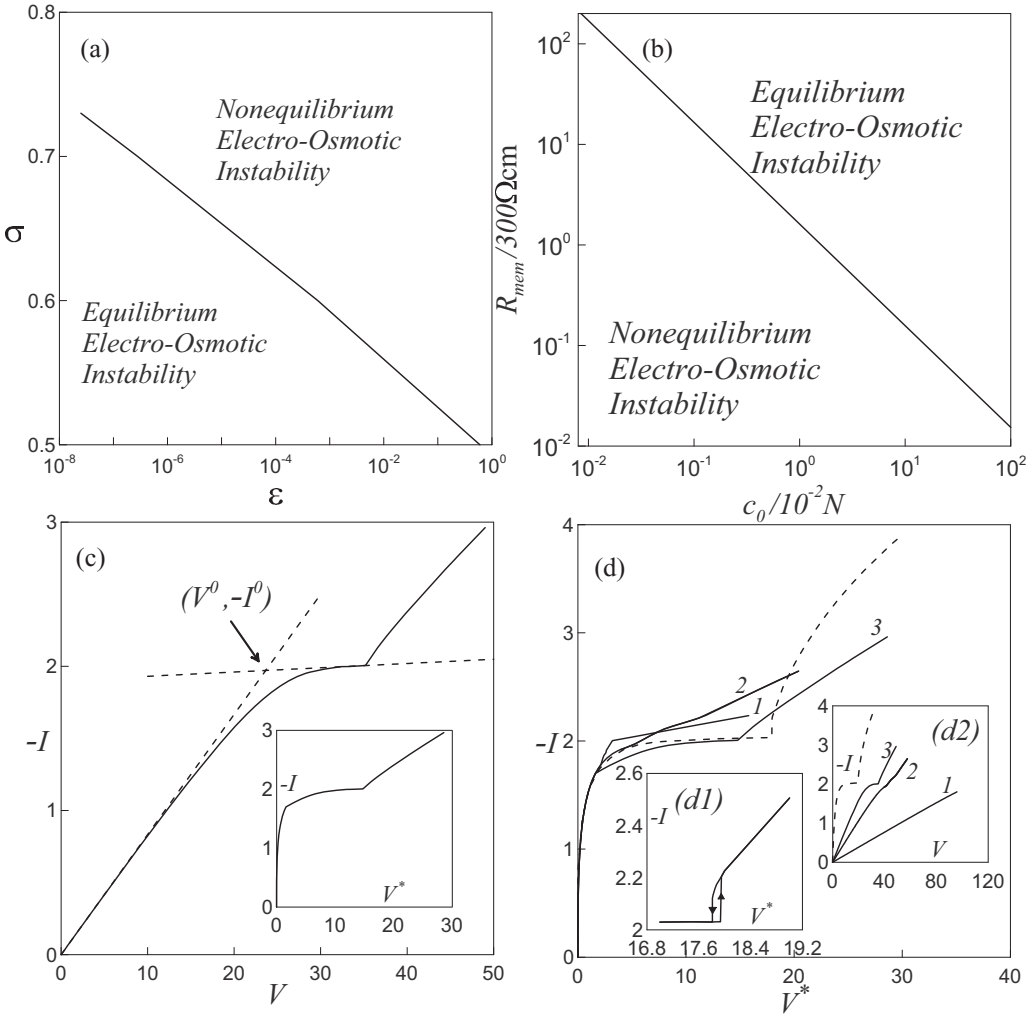

FIG. 3. Regions of domination of the two instability mechanisms in (a) the dimensionless conductivity–Debye length plane and (b) the dimensional membrane resistivity–electrolyte concentration plane. (As a prototypical example, an aqueous solution of copper sulfate is considered with $4M$ concentration of fixed charges in the membrane, with a membrane width of 500 μm and diffusion layer width of 100 μm.) (c) Normalizing procedure for voltage. The voltage-current dependence is approximated by two straight lines tangent to the linear initial part and the limiting current plateau. The normalized voltage is defined as $V^* = V - \min(dV/dI|_{I=0} I, V_0)$. The voltage-current dependence is for $L = 5$, $\sigma = 0.5$, and $N = 100$. The inset shows the same for normalized voltage. (d) Normalized voltage-current dependence for $L = 5$, $N = 100$, and $\sigma = 0.1$ (curve 1), $\sigma = 0.3$ (curve 2), and $\sigma = 0.5$ (curve 3). The dashed line shows the same dependence for a perfectly permselective membrane with infinite conductivity for $N = 100$ and $\varepsilon = 2.5 \times 10^{-4}$. The insets show (d1) the hysteresis loop in the voltage-current dependence magnified for a perfectly permselective membrane with infinite conductivity and (d2) the same dependence as in (d) for non-normalized voltage.

the range of 10^2–10^3 μm, and for the electrolyte concentration varying in the range of $10^{-3}N$–$10^{-1}N$. As shown in Fig. 3, both equilibrium and nonequilibrium electro-osmotic mechanisms coexist for the same voltage range. In order to determine which of the two mechanisms dominates the hydrodynamic instability and the resulting fluid flow we compare the value of the instability threshold for the normalized voltage for concentration polarization in the following two setups: (i) a perfectly permselective

cation-exchange membrane of finite conductivity and (ii) a perfectly permselective membrane of infinite conductivity, with $N \gg 1$ and $D = O(1)$. In the latter case the instability and the resulting fluid flow are solely mediated by the nonequilibrium electro-osmosis [12,14]. This latter situation is modeled by the full nonelectroneutral Nernst-Planck-Poisson-Stokes formulation in which the governing equations (1), (2), and (9) are complemented by the Poisson equation for the electric potential

$$\varepsilon^2 \nabla^2 \varphi = c_- - c_+ \tag{20}$$

and by the following boundary conditions at the membrane–depleted diffusion layer interface M-D^-, with $y = 0$:

$$c_{-y} - c_- \varphi_y = 0, \quad c_+ = N, \quad \varphi = -V, \quad \mathbf{v} = 0. \tag{21}$$

According to (21), vanishing of the co-ion flux is complemented by setting the interface counterion concentration equal to the fixed charge density in the membrane and assuming that the potential drops across the membrane M and the enriched layer D^+ are negligible compared to those over the depleted layer D^-; this is complemented by the no-slip condition for velocity. In Figs. 3(a) and 3(b) we depict the regions of domination of the two instability mechanisms in the dimensionless conductivity–Debye length plane [Fig. 3(a)] and in the dimensional membrane resistance–electrolyte concentration plane [Fig. 3(b)]. The decrease of bulk concentration yields domination of the nonequilibrium electro-osmotic mechanism over the equilibrium one. The contribution of the equilibrium mechanism increases with the increase of membrane resistivity. The linear stability analysis [Figs. 2(b)–2(d), 3(a) and 3(b)] of the limiting equilibrium model problem (5)–(11) was complemented by its nonlinear numerical solution. For this purpose we employed a suitably modified version of our previously developed FORTRAN finite-differences code [10]. The results of this solution were compared with those for the previously reported nonequilibrium model problem for a perfectly permselective membrane with infinite conductivity [10]. In terms of the voltage-current dependence, increasing the membrane conductivity σ results in a widening of the limiting current plateau and a subsequent increase of the slope in the overlimiting range [Figs. 3(c) and 3(d)]. This increase, upon the transition from the domination of the equilibrium mechanism to the nonequilibrium one, culminates in switching from a supercritical to subcritical bifurcation [Fig. 3(d1)] and its related critical jump (hysteresis loop) in the voltage-current curve. This transition from a smooth to a discontinuous voltage-current dependence depicted in Fig. 3(d) may be viewed as one of characteristic signatures of the instability mechanisms to be identified in the experiments. These two types of voltage-current dependences, smooth and discontinuous, have been observed experimentally for a long time for various types of ion-exchange membrane and microfluidic setups [6,9,10,33].

Another characteristic signature of the nonequilibrium mechanism is strong asymmetry of the critical vortices forming at the instability threshold accompanied by singular jet streams emanating at the ascending sides of the vortex pairs. In Figs. 4(a) and 4(c) we compare the flow streamlines and the corresponding concentration fields for the same value of normalized voltage for the two prototypical setups. The first is the limiting equilibrium model problem (5)–(11) for a perfectly permselective membrane with finite conductivity with the effect of the extended space charge disregarded. The sole driving mechanism for the instability in this case is the equilibrium electro-osmotic slip. The second is the nonequilibrium model corresponding to the full one-layer nonelectroneutral Nernst-Planck-Poisson-Stokes formulation for a perfectly permselective membrane with infinite conductivity, with $N \gg 1$ and $D = O(1)$.

We note the formation of a highly depleted region around the singular jet in the nonequilibrium case [Figs. 4(c) and 4(d)], also observed in the nonlinear numerical simulations in the one-layer Nernst-Planck-Poisson-Stokes setup [5,10,34,35]. In addition, the quadratic dependence of the slip velocity on the potential drop across the EDL in the nonequilibrium instability regime yields a much higher slip velocity compared to that in the equilibrium case [Fig. 4(e)] and manifests itself in a steeper voltage-current dependence.

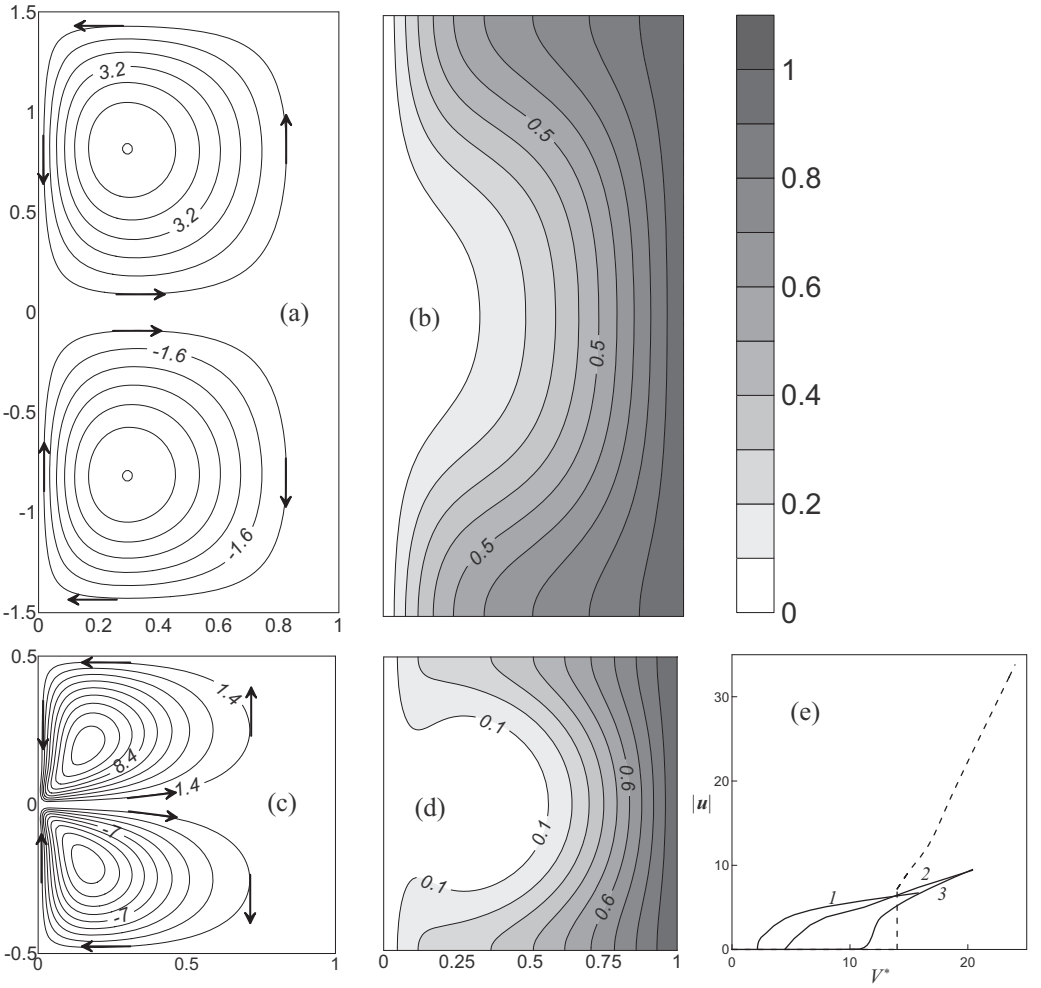

FIG. 4. (a) and (b) Flow streamlines and concentration distribution (darker color corresponds to higher concentration) in the depleted diffusion layer D^- computed for a perfectly permselective membrane with finite conductivity, for $L = 5$, $N = 100$, $\sigma = 0.5$, and $V^* = 20$. (c) and (d) Same for a perfectly permselective membrane with infinite conductivity computed for $N = 100$, $\varepsilon = 2.5 \times 10^{-4}$, and $V^* = 20$. (e) Dependence of the average flow velocity in the depleted layer on the normalized voltage for $L = 5$, $N = 100$, and $\sigma = 0.1$ (curve 1), $\sigma = 0.3$ (curve 2), and $\sigma = 0.5$ (curve 3). The dashed line shows the same dependence for a perfectly permselective membrane with infinite conductivity for $N = 100$ and $\varepsilon = 2.5 \times 10^{-4}$.

IV. CONCLUSION

The switching from supercritical to subcritical bifurcation accompanied by discontinuity of the voltage-current dependence and vortex asymmetry and jetting at the ascending part of the instability vortex are the characteristic signatures of the nonequilibrium instability mechanism as opposed to the equilibrium one. The proposed model of ionic transport through a perfectly permselective membrane with finite conductivity offers a convenient theoretical platform for a comparative investigation of both equilibrium and nonequilibrium instability mechanisms for realistic highly permselective systems. A thorough experimental analysis of the vicinity of the instability threshold, in terms of both voltage-current dependence and flow visualization, is required in order to determine the actual instability mechanism in a specific system.

[1] I. Rubinstein and B. Zaltzman, Equilibrium Electroconvective Instability, Phys. Rev. Lett. **114**, 114502 (2015).
[2] E. K. Zholkovskij, M. A. Vorotynsev, and E. Staude, Electrokinetic instability of solution in a plane-parallel electrochemical cell, J. Colloid Interface Sci. **181**, 28 (1996).
[3] R. Kwak, V. S. Pham, K. M. Lim, and J. Han, Shear Flow of an Electrically Charged Fluid by ion Concentration Polarization: Scaling Laws for Electroconvective Vortices, Phys. Rev. Lett. **110**, 114501 (2013).
[4] C. L. Druzgalski, M. B. Andersen, and A. Mani, Direct numerical simulation of electroconvective instability and hydrodynamic chaos near an ion-selective surface, Phys. Fluids **25**, 110804 (2013).
[5] E. A. Demekhin, N. V. Nikitin, and V. S. Shelistov, Direct numerical simulation of electrokinetic instability and transition to chaotic motion, Phys. Fluids **25**, 122001 (2013).
[6] H. C. Chang, G. Yossifon, and E. A. Demekhin, Nanoscale electrokinetics and microvortices: How microhydrodynamics affects nanofluidic ion flux, Annu. Rev. Fluid Mech. **44**, 401 (2012).
[7] H. C. Chang, E. A. Demekhin, and V. S. Shelistov, Competition between Dukhin's and Rubinstein's electrokinetic modes, Phys. Rev. E **86**, 046319 (2012).
[8] A. S. Khair, Concentration polarization and second-kind electrokinetic instability at an ion-selective surface admitting transverse flow, Phys. Fluids **23**, 072003 (2011).
[9] G. Yossifon and H. C. Chang, Selection of Nonequilibrium Overlimiting Currents: Universal Depletion Layer Formation Dynamics and Vortex Instability, Phys. Rev. Lett. **101**, 254501 (2008).
[10] S. M. Rubinstein, G. Manukyan, A. Staicu, I. Rubinstein, B. Zaltzman, R. G. H. Lammertink, F. Mugele, and M. Wessling, Direct Observation of a Nonequilibrium Electro-Osmotic Instability, Phys. Rev. Lett. **101**, 236101 (2008).
[11] E. V. Dydek, B. Zaltzman, I. Rubinstein, D. S. Deng, A. Mani, and M. Z. Bazant, Overlimiting Current in a Microchannel, Phys. Rev. Lett. **107**, 118301 (2011).
[12] I. Rubinstein and B. Zaltzman, in *Surface Chemistry and Electrochemistry of membranes*, edited by T. S. Sorensen (Dekker, New York, 1999).
[13] I. Rubinstein and B. Zaltzman, Electro-osmotically induced convection at a permselective membrane, Phys. Rev. E **62**, 2238 (2000).
[14] B. Zaltzman and I. Rubinstein, Electro-osmotic slip and electroconvective instability, J. Fluid Mech. **579**, 173 (2007).
[15] W. H. Smyrl and J. Newman, Double layer structure at the limiting current, Trans. Faraday Soc. **63**, 207 (1967).
[16] I. Rubinstein and L. Shtilman, Voltage against current curves of cation exchange membranes, J. Chem. Soc. Faraday Trans. II **75**, 231 (1979).
[17] M. Z. Bazant, K. T. Chu, and B. J. Bayly, Current-voltage relations for electrochemical thin films, SIAM J. Appl. Math. **65**, 1463 (2005).
[18] I. Rubinstein and B. Zaltzman, Dynamics of extended space charge in concentration polarization, Phys. Rev. E **81**, 061502 (2010).
[19] V. G. Levich, *Physicochemical Hydrodynamics* (Prentice Hall, Englewood Cliffs, 1962).
[20] B. M. Grafov and A. A. Chernenko, The theory of the passage of direct current through a solution of a binary electrolyte, Dokl. Akad. Nauk SSSR **146**, 135 (1962).
[21] R. P. Buck, Steady-state space-charge effects in symmetric cells with concentration polarized electrodes, J. Electroanal. Chem. **46**, 1 (1973).
[22] A. V. Listovnichy, Passage of currents higher than the limiting one through the electrodeelectrolyte solution system, Elektrokhimia **25**, 1651 (1989).
[23] V. V. Nikonenko, V. I. Zabolotsky, and N. P. Gnusin, Electric transport of ions through diffusion layers with impaired electroneutrality, Sov. Electrochem. **25**, 262 (1989).
[24] R. Kwak, G. Guan, W. K. Peng, and J. Han, Microscale electrodialysis: Concentration profiling and vortex visualization, Desalination **308**, 138 (2013).
[25] V. V. Nikonenko, A. V. Kovalenko, M. K. Urtenov, N. D. Pismenskaya, J. Han, P. Sistat, and G. Pourcelly, Desalination at overlimiting currents: State-of-the-art and perspectives, Desalination **342**, 85 (2014).

[26] I. Rubinstein, Electroconvection at an electrically inhomogeneous permselective interface, Phys. Fluids A **3**, 2301 (1991).
[27] E. A. Demekhin, S. Amiroudine, G. S. Ganchenko, and N. Y. Khasmatulina, Thermoelectroconvection near charge-selective surfaces, Phys. Rev. E **91**, 063006 (2015).
[28] I. Rubinstein and B. Zaltzman, Electro-osmotic slip of the second kind and instability in concentration polarization at electrodialysis membranes, Math. Mod. Methods Appl. Sci. **11**, 263 (2001).
[29] I. Rubinstein, B. Zaltzman, J. Pretz, and C. Linder, Experimental verification of the electroosmotic mechanism of overlimiting conductance through a cation exchange electrodialysis membrane, Russ. Electrochem. **38**, 853 (2002).
[30] I. Rubinstein and B. Zaltzman, Wave number selection in a nonequilibrium electro-osmotic instability, Phys. Rev. E **68**, 032501 (2003).
[31] S. S. Dukhin and B. V. Derjaguin, *Electrophoresis* (Nauka, Moscow, 1976).
[32] R. Abu-Rjal, I. Rubinstein, and B. Zaltzman, Driving factors of electro-convective instability in concentration polarization, Phys. Rev. Fluids **1**, 023601 (2016).
[33] F. Maletzki, H. W. Rösler, and E. Staude, Ion transfer across electrodialysis membranes in the overlimiting current range stationary voltage current characteristics and current noise power spectra under different conditions of free convection, J. Membr. Sci. **71**, 105 (1992).
[34] V. S. Pham, Z. Li, K. M. Lim, J. K. White, and J. Han, Direct numerical simulation of electroconvective instability and hysteretic current-voltage response of a permselective membrane, Phys. Rev. E **86**, 046310 (2012).
[35] C. Druzgalski and A. Mani, Statistical analysis of electroconvection near an ion-selective membrane in the highly chaotic regime, Phys. Rev. Fluids **1**, 073601 (2016).